

**Numerical computations of complexification of  
Legendrian knots.**

by

Bauyrzhan Yerzhibit

Submitted to the Department of Mathematics  
in partial fulfillment of the requirements for the degree of

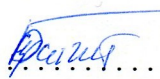
Master of Science in Mathematics

at the

NAZARBAYEV UNIVERSITY

Apr 2019

© Nazarbayev University 2019. All rights reserved.

Author .....  .....

Department of Mathematics

Apr 30, 2019

Certified by .....  .....

Mark Lawrence

Associate Professor

Thesis Supervisor

Accepted by .....

Vassilios D. Tourassis

Dean, School of Science and Technology

# Numerical computations of complexification of Legendrian knots.

Bauyrzhan Yerzhigit

April, 2019

## Abstract

With the recent interest in knots, it is interesting to study their complexification. We have chosen to study Legendrian knots as they have the property that we can reconstruct the original knot from its projection. This property is especially useful in the case of the complexification of a knot as in this case the diagram of the projection of the knot is no longer real. In this paper we show a way to compute complex rational functions that have a Legendrian knot as an image under unit circle.

## 1 Introduction

The study of knots began over a century ago and studied by mathematicians ever since. Recently, there has been increasing interest among physicists in studying knots. For example, a light field in 3 dimensional space can contain lines of zero intensity, in other words lines of darkness. Dennis et al. prove theoretically and experimentally the existence of knotted vortex loops in light fields [1]. The importance of these knotted nodal lines is that they "determine the topology of the wave field in space" [1]. Moreover, Dennis et al. states that the global topology of such a knotted vortex field is non-trivial and that such phenomena can be found in other three-dimensional wave systems [1]. Kleckner and Irvine show that they experimentally constructed isolated vortex knots and links in water [2]. They claim that "there is a growing realization that knots in space-filling fields are an essential part of physical processes" [2]. The connection between topology of knots and topology

of magnetic lines that were created by knotted wires are studied in [3] and [4] shows application of it. In [5], solutions to Maxwell's equation with knots that are preserved in time are constructed. Similarly, Enciso and Peralta-Salas show that "there exist steady solution to Euler equation in  $\mathbb{R}^3$  with vortex tubes of knots and links of any type" [6]. Etnyre and Ghrist have similar results for Euler equation on a Riemannian  $S^3$  in [7]. The papers [8] and [9] also contain recent studies about knots in optics and in electromagnetism.

Dennis and Bode shows a way to compute polynomials for a knot [10]. These polynomials  $f : S^3 \rightarrow \mathbb{C}$  have preimage of zero as the given knots. Their computations involve using Fourier series. The functions that are found in this way can be embedded into initial conditions for many physical systems [10]. Similarly, in [11] and [12], complex-valued eigenfunctions with nodal sets as knots are constructed.

There exists a large body of literature on the mathematical theory of knots, [13] is a classical reference, while [14] and [15] are recent ones.

## 1.1 Introducing Legendrian knots and its invariants

Let  $f : X \rightarrow Y$  be a function between two topological spaces, then it is called homeomorphism if it is continuous bijection and it has continuous inverse  $f^{-1}$ . A knot is a subset  $K$  of space  $X$  that is homeomorphic with a sphere  $S^p$ . If  $K$  is homeomorphic with disjoint union of one or more spheres then it is called a link [13].

Now to introduce Legendrian knots we have to define what is contact structure. A contact structure on an oriented 3-manifold  $M$  is a completely non-integrable plane field  $\xi$  in the tangent bundle of  $M$  [16]. A plane field is a smoothly varying family of planes, analogous to a vector field. A Legendrian curve is tangent to the plane at every point. The contact structure that we will be using is standard contact structure on  $\mathbb{R}^3$ ,  $\xi_{std}$ . It is a kernel of 1-form  $\alpha = dz - ydx$ .

A Legendrian knot  $L$  in a contact manifold  $(M^3, \xi)$  is embedded  $S^1$  that is always tangent to  $\xi$  [16]. This is an active research area, [17] and [18] are survey papers for reference.

A knot invariant is a function that assigns to each knot an object such that equivalent knots have same invariant. For Legendrian knots the equivalence is isotopy. Two Legendrian knots  $L_0$  and  $L_1$  are Legendrian isotopic if there is a continuous family  $L_t$ ,  $t \in [0, 1]$ , of Legendrian knots

starting at  $L_0$  and ending at  $L_1$ . Knot invariants are useful not just to distinguish knots but they also help to understand some properties of knots. These are classical invariants of Legendrian knots:

Thurston - Bennequin number: Let  $v$  be a non-zero vector field along  $L$  transverse to  $\xi$  and let  $L'$  be a copy of  $L$  obtained by pushing  $L$  slightly in the direction of  $v$ . Then Thurston - Bennequin number is the linking number of  $L$  and  $L'$  [16].

Rotation number: Let  $v$  be vector field tangent to  $L$  and pointing in a direction of orientation of  $L$ . The rotation number of  $L$  is the winding number of  $v$ , by thinking of  $v$  as a path of non-zero vectors in  $\mathbb{R}^2$  [16].

In [19], Chekanov showed that some Legendrian knots with the same classical invariants are not Legendrian isotopic to each other by developing his own invariant, in which he used contact homology. So, contact homology distinguishes Legendrian knots. In his paper, Chekanov used two  $5_2$  knots to prove it, so we have done computations for these two knots.

## 1.2 Complexification of Legendrian knots

Complexification is the process of replacing real variables by complex variables in equations. Here we are using a geometric analogue, so that curves in 3 dimensional real space are "complexified" into complex surfaces in 3-dimensional complex space. In terms of real dimensions, this corresponds to a 2 dimensional surface in  $R^6$ . There are several recent studies in the direction of complex Legendrian knots, such us [20], [21] and [22].

When we complexify the diagram disappears and we cannot find usual invariants. Now, we are trying to get the information about invariants of knots in different ways. The crossing points and cusps still make sense, so we can find them by studying the polynomials.

The purpose of this research is to study complexification of Legendrian knots. We hope that this will help us to understand the invariants of Legendrian knots with complexifications. For example, we want to count the number of complex crossing points and cusps and try to determine any mathematical significance.

We do this by finding complex polynomials which have knots as images of  $S^1$ . Particularly, our goal is to find polynomials whose images are the trefoil and  $5_2$  knots. The method is to build

a system of equations which include two complex rational functions and their derivatives. Then, we solve them using numerical tools and generate 2D figures and possibly 3D.

In our approach we want to find two polynomials  $P$  and  $Q$  such that the intersection of their zero sets give us Legendrian knots. However, we start by finding parametric polynomials for  $x$  and  $z$ , while  $y$  will follow from properties of Legendrian front projection. In this paper we show how to do the computations for trefoil knot. The results of the computations for  $4_1$  knot,  $5_1$  knot and two  $5_2$  knots are given at the end of the paper. Theoretically this scheme can be applied to any Legendrian knot, although for knots that require higher degree of polynomials there may be issues with numerical errors.

## 2 Mathematical justification for the method

In this section we will prove that the image of our complex rational map is a variety. Legendrian curves are defined by the contact form  $dz - ydx$ , which becomes zero when you plug in the parametric real curve. This equation will also be valid for complex analytic maps as well. Let  $(x(t), z'(t)/x'(t), z(t))$  be the rational map on the  $\mathbb{C} \setminus \{0\}$ . First, we prove that this map is analytic by showing that each component is complex analytic. We want a function which is real valued on the unit circle. Because of the reflection principle with  $z$  maps to  $\overline{1/\bar{z}}$ , such a function must have the form  $\sum_{j=1}^n (a_j t^j + \bar{a}_j t^{-j})$ , which we see is real valued on the unit circle. If we use conjugation and reflection we will have:

$$\overline{p\left(\frac{1}{\bar{t}}\right)} = \overline{\sum_{j=1}^n \left(a_j \left(\frac{1}{\bar{t}}\right)^j + \bar{a}_j \left(\frac{1}{\bar{t}}\right)^{-j}\right)} = \overline{\sum_{j=1}^n \left(a_j (\bar{t})^{-j} + \bar{a}_j (\bar{t})^j\right)} = \sum_{j=1}^n \left(\bar{a}_j (t)^{-j} + a_j (t)^j\right) = p(t). \quad (1)$$

Next, we will show that the map is real for all  $t$  from unit circle. We will use the fact that  $t^{-1} = \bar{t}$  holds for a complex number  $t$  from  $S^1$ .

$$p(t) = \sum_{j=1}^n (a_j t^j + \bar{a}_j \bar{t}^j) = \sum_{j=1}^n 2\text{Re}(a_j t^j). \quad (2)$$

For  $z'(t)/x'(t)$  to be analytic we will define  $z(t) = p_2(t)$  such that it's first and second derivatives are equal to zero whenever  $x'(t) = 0$ . This way we will have complex "cusps" and  $z'(t)/x'(t)$  is analytic as a ratio of two analytic functions. We do not specifically force  $x''(t) \neq 0$  as in practice it will not become zero by itself. This can be seen from the graphs of knots that we have in this paper.

As a result, as we define the map  $(x(t), z'(t)/x'(t), z(t))$  such that it's image under  $S^1$  is a Legendrian knot, when we plug this map into the contact form  $dz - ydx$ , the result will be an analytic function which will be equal to zero on the unit circle. By uniqueness principle [23, p. 83], if a function is analytic in a given domain and it vanishes on a curve inside of this domain then it is equal to zero for all points in the domain. Thus, in this way we will have complexification of a Legendrian knot.

To show that the image of the map is an analytic variety, we use the theorem that the image

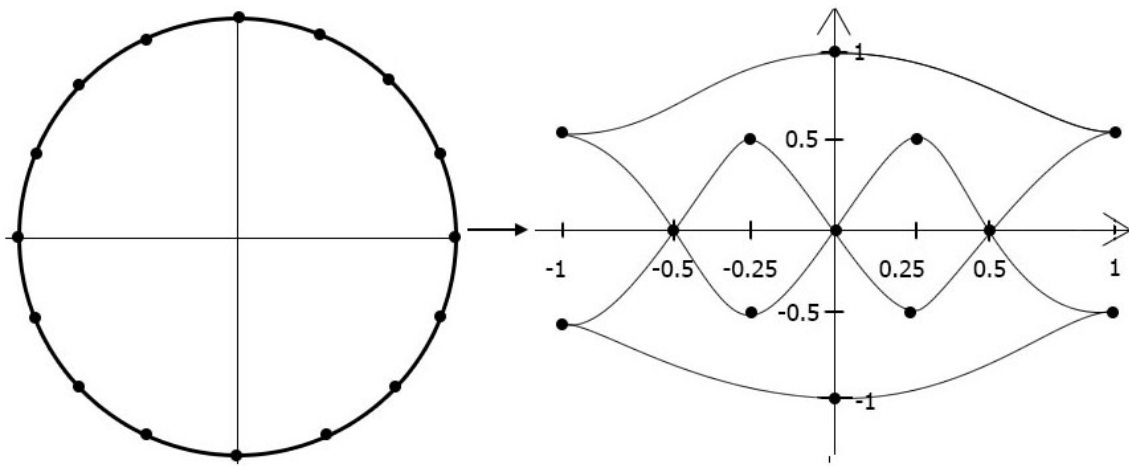
of a variety under a finite map is a variety. Finite map means that the pre-image of every point in the image is finite and since we have a rational map, finiteness is automatic.

Finally, we use corollary which states that a finite map takes Zariski closed sets to Zariski closed sets [24, p. 62]. In this context a closed set is an algebraic variety and the Riemann sphere is an algebraic variety. A rational map is finite and therefore the image is also a variety.

### 3 Methodology and preliminary results

First, we start with the graph of a Legendrian knot, then we try to approximate a function with image over  $S^1$  which is that graph. We take points where we have cusps, crosses and tangents and by using values of polynomial and its derivatives at these points try to compute the coefficients of the polynomials. The first knot that we will be studying is trefoil knot.

Figure 1: Map from  $S^1$  to trefoil knot



Equations of a polynomial for x:	
Equations for locations of cusps:	Equations for derivatives at cusps:
1. $x(e^{i\pi/8}) = -1$	5. $x'(e^{i\pi/8}) = 0$
2. $x(e^{i9\pi/8}) = -1$	6. $x'(e^{i7\pi/8}) = 0$
3. $x(e^{i7\pi/8}) = 1$	7. $x'(e^{i9\pi/8}) = 0$
4. $x(e^{i15\pi/8}) = 1$	8. $x'(e^{i15\pi/8}) = 0$
Equations for locations of crossings:	Equations for locations of horizontal tangents:
9. $x(e^{i2\pi/8}) = -1/2$	15. $x(e^{i3\pi/8}) = -1/4$
10. $x(e^{i10\pi/8}) = -1/2$	16. $x(e^{i5\pi/8}) = 1/4$
11. $x(e^{i4\pi/8}) = 0$	17. $x(e^{i8\pi/8}) = 0$
12. $x(e^{i12\pi/8}) = 0$	18. $x(e^{i11\pi/8}) = -1/4$
13. $x(e^{i6\pi/8}) = 1/2$	19. $x(e^{i13\pi/8}) = 1/4$
14. $x(e^{i14\pi/8}) = 1/2$	20. $x(e^{i16\pi/8}) = 0$

Equations of a polynomial for z:		
Equations for locations of cusps:	Equations for derivatives at cusps:	
1. $z(e^{i\pi/8}) = 1/2$	5. $z'(e^{i\pi/8}) = 0$	9. $z''(e^{i\pi/8}) = 0$
2. $z(e^{i9\pi/8}) = -1/2$	6. $z'(e^{i7\pi/8}) = 0$	10. $z''(e^{i7\pi/8}) = 0$
3. $z(e^{i7\pi/8}) = 1/2$	7. $z'(e^{i9\pi/8}) = 0$	11. $z''(e^{i9\pi/8}) = 0$
4. $z'(e^{i15\pi/8}) = -1/2$	8. $z'(e^{i15\pi/8}) = 0$	12. $z''(e^{i15\pi/8}) = 0$
Equations for locations of crossings:	Equations for locations of horizontal tangents:	Equations for derivatives at horizontal tangents:
13. $z(e^{i2\pi/8}) = 0$	19. $z(e^{i3\pi/8}) = -1/2$	25. $z'(e^{i3\pi/8}) = 0$
14. $z(e^{i10\pi/8}) = 0$	20. $z(e^{i5\pi/8}) = 1/2$	26. $z'(e^{i5\pi/8}) = 0$
15. $z(e^{i4\pi/8}) = 0$	21. $z(e^{i8\pi/8}) = -1$	27. $z'(e^{i8\pi/8}) = 0$
16. $z(e^{i12\pi/8}) = 0$	22. $z(e^{i11\pi/8}) = 1/2$	28. $z'(e^{i11\pi/8}) = 0$
17. $z(e^{i6\pi/8}) = 0$	23. $z(e^{i13\pi/8}) = -1/2$	29. $z'(e^{i13\pi/8}) = 0$
18. $z(e^{i14\pi/8}) = 0$	24. $z(e^{i16\pi/8}) = 1$	30. $z'(e^{i16\pi/8}) = 0$

We assume that

$$x(t) = p_1(t) = \sum_{j=1}^8 (a_j t^j + \bar{a}_j t^{-j}). \quad (3)$$

This polynomial will be real valued on unit circle,  $S^1$ . As we are finding image of this polynomial over  $S^1$ , we can assume that  $t^{-j} = \bar{t}^j$ . Then, we have

$$p_1(t) = \sum_{j=1}^8 (a_j t^j + \bar{a}_j \bar{t}^j) = \sum_{j=1}^8 2\operatorname{Re}(a_j t^j). \quad (4)$$

Now, we can write  $a_j$  as sum of real and imaginary parts. Let us denote them as  $\alpha_j$  and  $\beta_j$ , respectively. Because  $t$  is on  $S^1$ , we can write it as  $t = \cos\theta + i\sin\theta$ . Then, on  $S^1$  (2) becomes

$$p_1(t) = \sum_{j=1}^8 2\operatorname{Re}[(\alpha_j + i\beta_j)(\cos j\theta + i\sin j\theta)] = \sum_{j=1}^8 2(\alpha_j \cos j\theta - \beta_j \sin j\theta). \quad (5)$$

Now, we turn to equations with  $x'$ . From (1) we get

$$x'(t) = p'_1(t) = \sum_{j=1}^8 (a_j j t^{j-1} - \bar{a}_j j t^{-j-1}). \quad (6)$$

As we are taking values of  $t$  on  $S^1$  we have

$$\begin{aligned} p'_1(t) &= \sum_{j=1}^8 (a_j j t^{j-1} - \bar{a}_j j \bar{t}^{j+1}) \\ &= \sum_{j=1}^8 j [(\alpha_j + i\beta_j)(\cos((j-1)\theta) + i\sin((j-1)\theta)) - (\alpha_j - i\beta_j)(\cos((j+1)\theta) - i\sin((j+1)\theta))]. \end{aligned} \quad (7)$$

Now, to solve the equations  $p'_1(t) = 0$  we solve real and imaginary parts separately. Thus, we will get two equations for each cusp.

$$\begin{cases} \sum_{j=1}^8 j [\alpha_j (\cos((j-1)\theta) - \cos((j+1)\theta)) + \beta_j (-\sin((j-1)\theta) + \sin((j+1)\theta))] = 0. \\ \sum_{j=1}^8 j [\alpha_j (\sin((j-1)\theta) + \sin((j+1)\theta)) + \beta_j (\cos((j-1)\theta) + \cos((j+1)\theta))] = 0. \end{cases}$$

Then, we do similar process for  $z$ . As the number of equation for  $z$  is bigger than for  $x$ , we

need polynomial of higher degree.

$$z(t) = p_2(t) = \sum_{j=1}^{11} (b_j t^j + \bar{b}_j t^{-j}). \quad (8)$$

The equations for  $z$  and  $z'$  are calculated in the same way as for  $x$ . In addition, as we have to solve equation with  $z''$ , we calculate polynomial's second derivative. From (7) we get

$$z''(t) = p_2''(t) = \sum_{j=2}^{11} (b_j(j)(j-1)t^{j-2} + \sum_{j=1}^{11} \bar{b}_j(j)(j+1)t^{-j-2}). \quad (9)$$

As we are taking values of  $t$  on  $S^1$  we have

$$\begin{aligned} p_1''(t) = & \sum_{j=2}^{11} [(\alpha_j + i\beta_j)(j)(j-1)(\cos((j-2)\theta) + i\sin((j-2)\theta))] \\ & + \sum_{j=1}^{11} [(\alpha_j - i\beta_j)(j)(j+1)(\cos((j+2)\theta) - i\sin((j+2)\theta))]. \end{aligned} \quad (10)$$

As previously, we solve equations for  $z''(t) = 0$  by solving real and imaginary parts separately. So, we have:

$$\left\{ \begin{array}{l} 2\alpha_1 \cos(3\theta) - 2\beta_1 \sin(3\theta) + \sum_{j=2}^{11} \{ \alpha_j [(j)(j-1)\cos((j-2)\theta) \\ + (j)(j+1)\cos((j+2)\theta)] + \beta_j [-(j)(j+1)\sin((j+2)\theta) - (j)(j-1)\sin((j-2)\theta)] \} = 0 \\ -2\alpha_1 \sin(3\theta) - 2\beta_1 \cos(3\theta) + \sum_{j=2}^{11} \{ \alpha_j [(j)(j-1)\sin((j-2)\theta) \\ - (j)(j+1)\sin((j-2)\theta)] + \beta_j [(j)(j-1)\cos((j-2)\theta) - (j)(j+1)\cos((j+2)\theta)] \} = 0 \end{array} \right.$$

At first we wanted to solve these equations exactly. We tried to take number of complex variables to be equal half of the equations, because the number of real unknowns would be equal to the number of equations. However, some equations were dependent on others and this caused almost singular system. Thus, we tried to take number of unknowns much less than number of equations and find least squares solution. By judging from the graphs of these solutions we adjusted the number of unknowns so that the graph looks similar to what we have expected.

The 2D graph of these polynomials is given below. Here we used 8 complex unknown coefficients for  $x$  polynomial and 13 complex unknown coefficients for  $z$  polynomial:

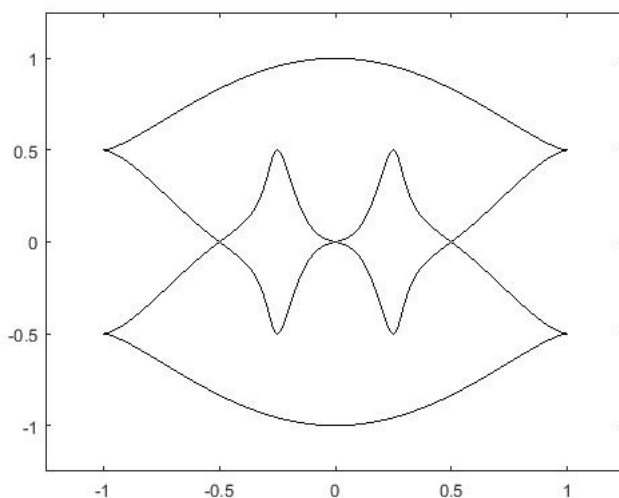


Figure 2: Graph of polynomials for trefoil knot

Next step is to add complex cusps to the constraints, because we have  $dz - ydx = 0$ . So, if  $dx = 0$  at some point, then we want  $dz = 0$  at that point. In order to do this, we find all the zeros of first derivative of polynomial for x-coordinate. Then, take the points outside of  $S^1$  and make first and second derivatives of polynomials for z-coordinate to be equal to zero at these points. The number of equations increased substantially as for each point there were two equations for first and second derivatives, which in turn were converted to two equations for each derivatives. Thus, it required us to use more unknowns. Although this method give us very similar graphs, the cusps were the issue. If we looked near these cusps we could see that they are not real cusps. This was caused by approximations and numerical errors.

The 2D graph of these polynomials is given below. Here we used 8 complex unknown coefficients for x polynomial and 19 complex unknown coefficients for z polynomial:

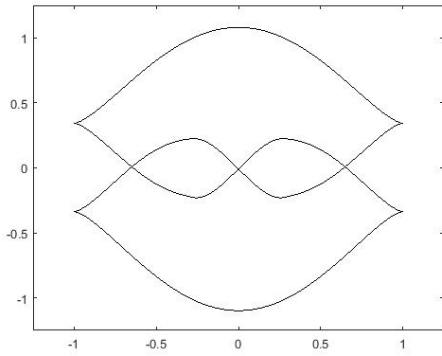


Figure 3: Graph of polynomials with complex cusps for trefoil knot

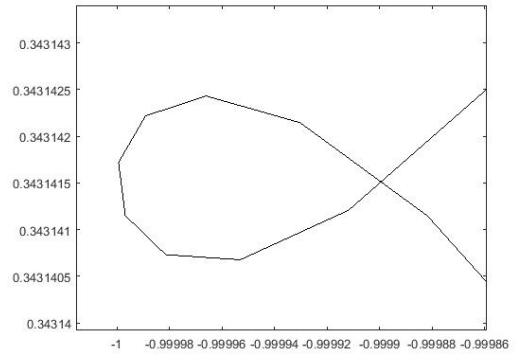


Figure 4: Near one of the cusps of the graph in figure 3

Then, we tried to take equations for real cusps involving derivatives as equality constraints and apply least squares method for other equations. These showed better results.

The 2D graph of these polynomials is given below. Here we used 8 complex unknown coefficients for x polynomial and 23 complex unknown coefficients for z polynomial:

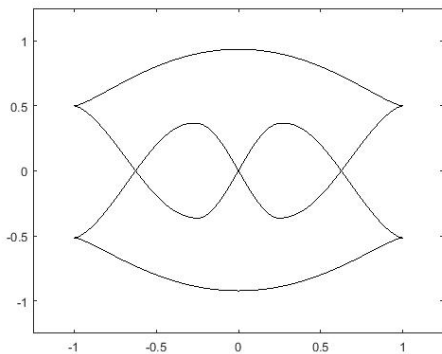


Figure 5: Graph of polynomials with complex cusps for trefoil knot

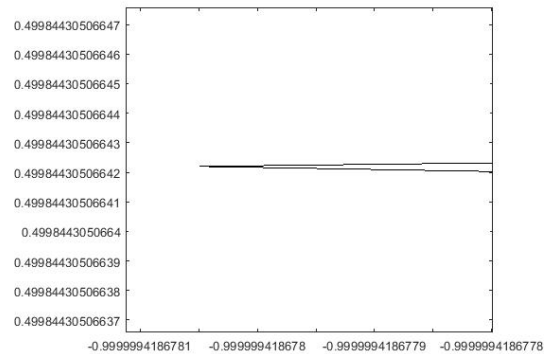


Figure 6: Near one of the cusps of the graph in figure 5

We tried to add the equations of complex cusps to the equality constraints, but they turned out to be inconsistent. Thus, we just tried to add them to other equations to be minimized. As a result, we do not really have complex cusps. The least squares solution gives us errors for each equation less than 0.2. This is not a too bad result considering that we have 76 equations to

minimize. The following polynomials are results of our computations for trefoil knot:

$$\begin{aligned}
x(t) = p_1(t) = & (-0.0103i)t^{-8} + (-0.096i)t^{-6} + (-0.1875i)t^{-4} + (-0.346i)t^{-2} \\
& + (0.346i)t^2 + (0.1875i)t^4 + (0.096i)t^6 + (0.0103i)t^8.
\end{aligned} \tag{11}$$

$$\begin{aligned}
z(t) = p_2(t) = & (0.0001)t^{-23} + (0.0014)t^{-21} + (0.0001)t^{-20} + (0.0052)t^{-19} + (-0.0003)t^{-18} \\
& + (0.0048)t^{-17} + (-0.0001)t^{-16} + (0.0056)t^{-15} + (0.0001)t^{-14} \\
& + (0.0065)t^{-13} + (0.0006)t^{-12} + (0.0501)t^{-11} + (-0.0013)t^{-10} \\
& + (0.0259)t^{-9} + (0.0001)t^{-8} + (0.0179)t^{-7} + (-0.0004)t^{-6} + (-0.0706)t^{-5} \\
& + (0.0019)t^{-4} + (0.2815)t^{-3} + (-0.0007)t^{-2} + (0.1487)t^{-1} \\
& + (0.1487)t + (-0.0007)t^2 + (0.2815)t^3 + (0.0019)t^4 \\
& + (-0.0706)t^5 + (-0.0004)t^6 + (0.0179)t^7 + (0.0001)t^8 + (0.0259)t^9 \\
& + (-0.0013)t^{10} + (0.0501)t^{11} + (0.0006)t^{12} + (0.0065)t^{13} \\
& + (0.0001)t^{14} + (0.0056)t^{15} + (-0.0001)t^{16} + (0.0048)t^{17} \\
& + (-0.0003)t^{18} + (0.0052)t^{19} + (0.0001)t^{20} + (0.0014)t^{21} + (0.0001)t^{23}.
\end{aligned} \tag{12}$$

For Legendrian knots we can reproduce entire knot from front projection. Because we have the relation  $dz - ydx = 0$ , we can find y coordinate by ratio  $y = dz/dx$ . Thus, in our case we have  $y = p'_2(t)/p'_1(t)$ .

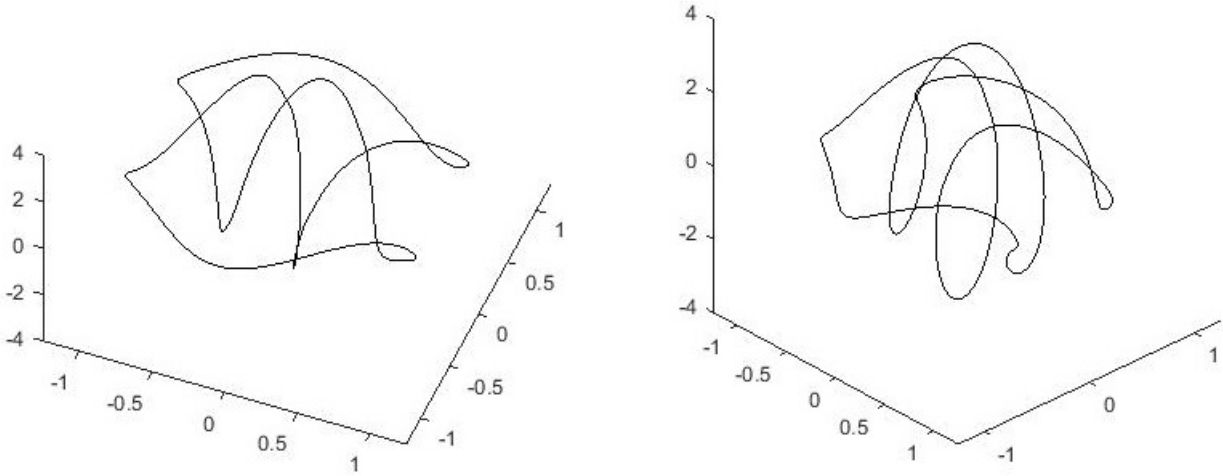


Figure 7: 3D plot of the knot given in figure 5

In addition to trefoil, we have repeated the process for  $4_1$ ,  $5_1$  and two  $5_2$  knots. Their graphs are given at the end of this paper. The increase of the number of equations made it harder to find correct number of unknowns for  $x$  and  $z$  polynomials. Moreover, adding complex cusps was impossible in these cases as adding them will give minimized solution whose graph was not our desired knot.

At last, when we have constructed polynomials  $x = p_1(t)$ ,  $y = p_2'(t)/p_1'(t)$  and  $z = p_2(t)$  for a given knot we attempt to find polynomials  $P(x, y, z)$  and  $Q(x, y, z)$  such that the intersection of their zero sets is graph of the knot. Theoretically this should be possible, however practically we just search for any polynomials that will give us the knot. We used software called "Singular" and tried to find these polynomials. The idea was to find polynomials that generate an ideal which is the kernel of the transformation:  $C[x, y, z] \rightarrow C[t]$  so that  $x \rightarrow p_1(t)$ ,  $y \rightarrow p_2'(t)/p_1'(t)$ ,  $z \rightarrow p_2(t)$ .

Unfortunately, this software was not able to find polynomials for trefoil and other knots. We assume that this is due to limitations of this software. The only knot for which this software could find polynomials is the unknot. The following is figure of the unknot and its polynomials:

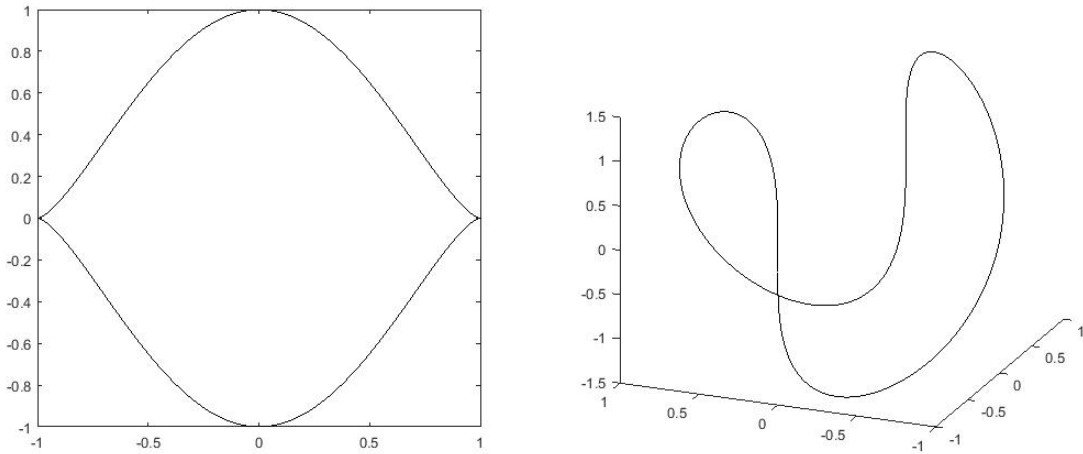


Figure 8: 2D and 3D plot of the unknot

$$\left\{ \begin{array}{l} x(t) = p_1(t) = -0.5t^{-1} - 0.5t. \\ z(t) = p_2(t) = (0.125i)t^{-3} + (-0.375i)t^{-1} + (0.375i)t + (-0.125i)t^3. \end{array} \right.$$

The following is set of polynomials that we have obtained using "Singular":

$$\left\{ \begin{array}{l} xyz - 3x^2 - 0.333333y^2 - 3z^2 + 3 \\ x^2y - 3xz - y \\ x^3 + 0.111111xy^2 - 0.333333yz - x \\ y^4 + 81x^2z^2 + 27xyz \\ xy^3 + 27x^2z - 3y^2z \end{array} \right.$$

So, we have 5 polynomials instead of 2, but this is still a good result.

## References

- [1] Mark R. Dennis, Robert P. King, Barry Jack, Kevin O'Holleran, Miles J. Padgett, "Isolated optical vortex knots," *Nature Physics* volume 6, pages 118121 (2010), DOI: 10.1038/NPHYS1504.
- [2] D. Kleckner und W. T. . M. Irvine, Creation and dynamics of knotted vortices, *Nature Physics*, p. 12-13, 03. Mrz 2013.
- [3] Alberto Enciso, Daniel Peralta-Salas, "A problem of Ulam about magnetic fields generated by knotted wires," Feb 2016. arXiv:1602.03142
- [4] S. R. Hudsona, E. Startsev, and E. Feibush, "A new class of magnetic confinement device in the shape of a knot," *Physics of Plasmas* 21, 010705 (2014); <https://doi.org/10.1063/1.4863844>
- [5] Hriday Kedia, Iwo Bialynicki-Birula, Daniel Peralta-Salas, and William T. M. Irvine, "Tying Knots in Light Fields," *Phys. Rev. Lett.* 111, 150404 Published 10 October 2013.
- [6] Alberto Enciso, Daniel Peralta-Salas, "Existence of knotted vortex tubes in steady Euler flows," Oct 2012. arXiv:1210.6271
- [7] John Etnyre, Robert Ghrist, "Contact topology and hydrodynamics III: knotted orbits", *Trans. Amer. Math. Soc.* 352 (2000), 5781-5794. DOI: <https://doi.org/10.1090/S0002-9947-00-02651-9>
- [8] A. S. Desyatnikov, D. Buccoliero, M. R. Dennis und Y. S. Kivshar, "Spontaneous knotting of self," *Scientific Reports*, p. 12-13, 25. Oct 2012.
- [9] Nikolay N. Rosanov, Nina V. Vysotina, Anatoly N. Shatsev, Anton S. Desyatnikov, and Yuri S. Kivshar, "Knotted Solitons in Nonlinear Magnetic Metamaterials," *Phys. Rev. Lett.* 108, 133902, March 2012.
- [10] Mark R Dennis, Benjamin Bode, "Constructing a polynomial whose nodal set is the three-twist knot  $5_2$ ", (Dec 2016), arXiv:1612.06801.

- [11] Alberto Enciso, David Hartley, Daniel Peralta-Salas, "Laplace operators with eigenfunctions whose nodal set is a knot," May 2015. arXiv:1505.06684
- [12] Alberto Enciso, David Hartley, Daniel Peralta-Salas, "A problem of Berry and knotted zeros in the eigenfunctions of the harmonic oscillator," May 2015. arXiv:1503.05101
- [13] Dale Rolfsen, *Knots and Links*, American Mathematical Society, 2003.
- [14] W. Menasco and M. Thistlethwaite, "Handbook of Knot Theory", Elsevier Science, 2005.
- [15] Louis H. Kauffman, "Formal Knot Theory", Courier Corporation, 2006.
- [16] John B. Etnyre, Legendrian and Transversal knots, Nov 2004. arXiv:math/0306256
- [17] John B. Etnyre, Ko, Honda, "Knots and Contact Geometry I: Torus Knots and the Figure Eight Knot," *J. Symplectic Geom.* 1 (2001), no. 1, 63–120.
- [18] John B. Etnyre, Lenhard L. Ng, Vera Vertesi, "Legendrian and transverse twist knots," Oct 2011. arXiv:1002.2400
- [19] Chekanov, Y. *Invent. math.* (2002) 150: 441. <https://doi.org/10.1007/s002220200212>
- [20] Jun-Muk Hwang, Keiji Ogiso, "Multiple fibers of holomorphic Lagrangian fibrations," Jul 2009. arXiv:0907.4869
- [21] Jun-Muk Hwang, Richard M. Weiss, "Webs of Lagrangian Tori in Projective Symplectic Manifolds," Jan 2012. arXiv:1201.2369
- [22] Jun-Muk Hwang, "Rigidity properties of holomorphic Legendrian singularities," May 2018. arXiv:1805.03349
- [23] J. Brown, R. Churchill, "Complex variables and applications", McGraw-Hill, 2009.
- [24] Shafarevich, Igor R, "Basic algebraic geometry", Springer, 2013.

## 4 Appendix

### 4.1 Graphs of polynomials for several knots which were calculated by the method that was used for trefoil knot.

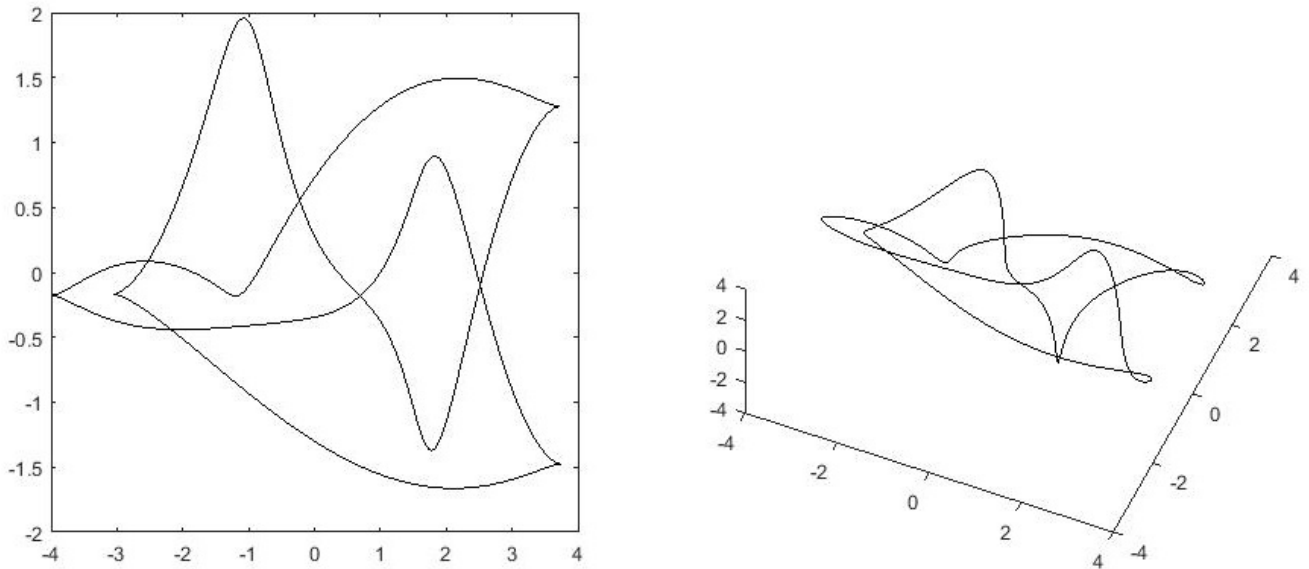


Figure 9: 2D and 3D graphs of the computed polynomials for  $4_1$  knot

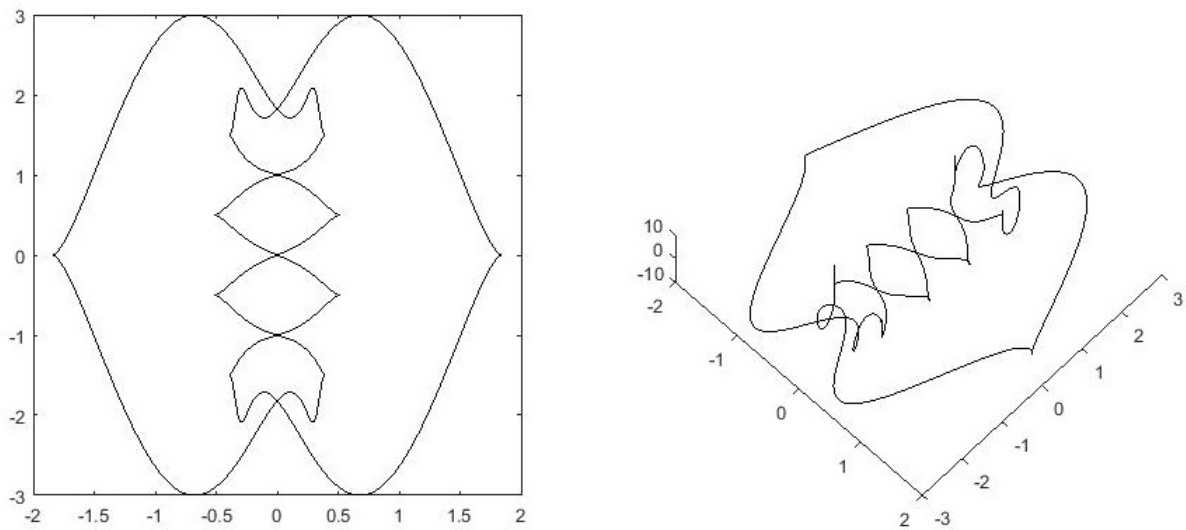


Figure 10: 2D and 3D graphs of the computed polynomials for  $5_1$  knot

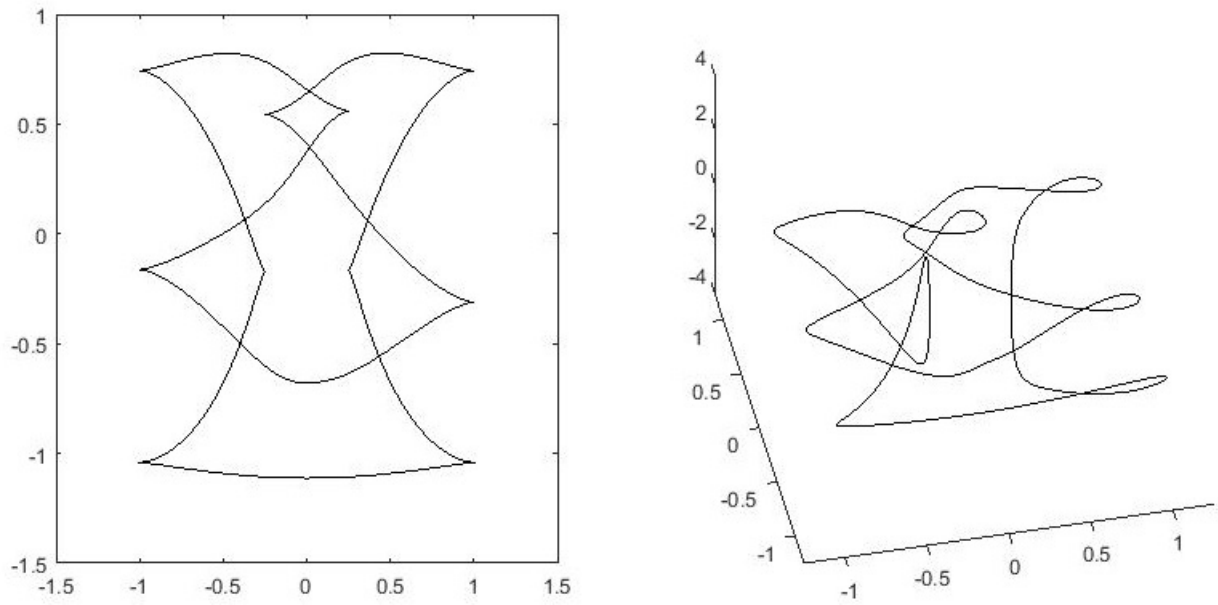


Figure 11: 2D and 3D graphs of the computed polynomials for  $5_2$  knot A

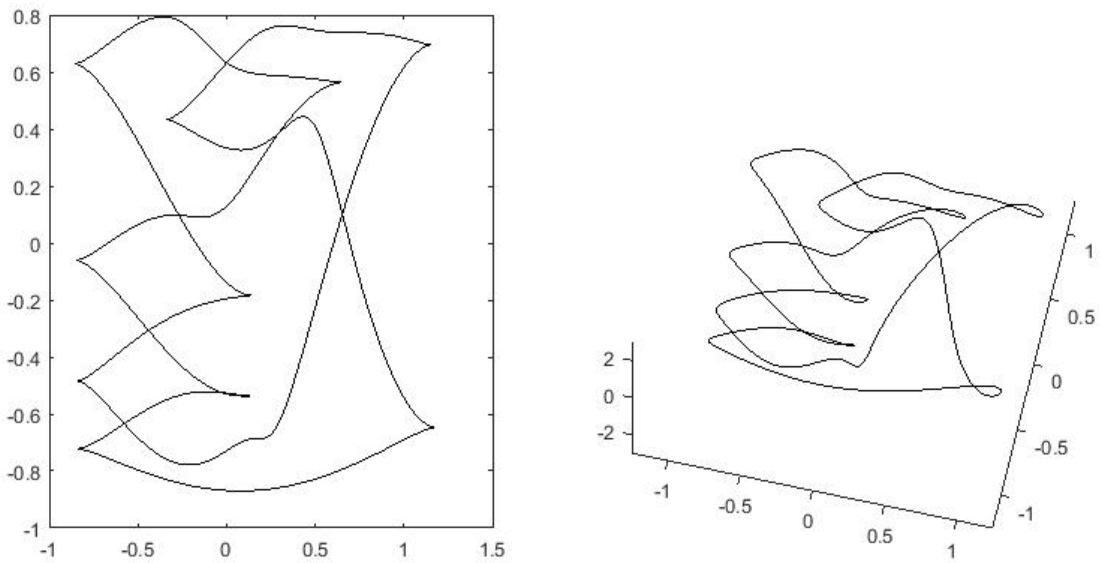


Figure 12: 2D and 3D graphs of the computed polynomials for  $5_2$  knot B

4.2 Coefficients of polynomials for several knots which were calculated by the method shown in this paper. Note that in these cases, the calculations did not include adding complex cusps.

Table 1: Coefficients of polynomials for  $4_1$  knot

coefficients for $p_1(t)$	coefficients for $p_2(t)$
$a_1 = -0.4536 + 0.0495i$	$b_1 = -0.0408 + 0.2764i$
$a_2 = -1.4075 - 0.5861i$	$b_2 = 0.0770 - 0.0323i$
$a_3 = -0.0345 + 0.2730i$	$b_3 = -0.3542 - 0.2181i$
$a_4 = 0.1888 - 0.0489i$	$b_4 = 0.2516 + 0.1486i$
$a_5 = -0.2979 + 0.0891i$	$b_5 = -0.0127 + 0.1763i$
$a_6 = -0.0709 + 0.1071i$	$b_6 = 0.0574 - 0.0940i$
$a_7 = 0.0603 - 0.1012i$	$b_7 = -0.0488 - 0.0291i$
$a_8 = 0.0239 + 0.0152i$	$b_8 = -0.0218 - 0.0130i$
	$b_9 = -0.0620 - 0.0264i$
	$b_{10} = 0.0895 + 0.0462i$
	$b_{11} = -0.0146 - 0.0036i$
	$b_{12} = -0.0085 - 0.0288i$

Table 2: Coefficients of polynomials for  $5_1$  knot

coefficients for $p_1(t)$	coefficients for $p_2(t)$
$a_1 = -0.2014$	$b_1 = 0$
$a_2 = 0$	$b_2 = -0.9175i$
$a_3 = -0.2190$	$b_3 = 0$
$a_4 = 0$	$b_4 = -0.4063i$
$a_5 = -0.3470$	$b_5 = 0$
$a_6 = 0$	$b_6 = -0.2214i$
$a_7 = -0.0327$	$b_7 = 0$
$a_8 = 0$	$b_8 = -0.1296i$
$a_9 = -0.0879$	$b_9 = 0$
$a_{10} = 0$	$b_{10} = -0.0875i$
$a_{11} = -0.0312$	$b_{11} = 0$
	$b_{12} = -0.0099i$
	$b_{13} = 0$
	$b_{14} = 0.0212i$
	$b_{15} = 0$
	$b_{16} = 0.0869i$
	$b_{17} = 0$
	$b_{18} = 0.1119i$
	$b_{19} = 0$
	$b_{20} = 0.0989i$
	$b_{21} = 0$
	$b_{22} = 0.0572i$
	$b_{23} = 0$
	$b_{24} = -0.0049i$

Table 3: Coefficients of polynomials for  $5_2$  knot A

coefficients for $p_1(t)$	coefficients for $p_2(t)$
$a_1 = -0.2415 + 0.0293i$	$b_1 = -0.0066 - 0.0914i$
$a_2 = -0.0182 - 0.0740i$	$b_2 = 0.4033 - 0.1082i$
$a_3 = 0.1727 - 0.0655i$	$b_3 = 0.0135 + 0.0591i$
$a_4 = -0.0692 - 0.1318i$	$b_4 = -0.0186 + 0.0201i$
$a_5 = -0.1116 + 0.0771i$	$b_5 = 0.0198 + 0.0140i$
$a_6 = -0.0879 - 0.0992i$	$b_6 = -0.0107 + 0.0035i$
$a_7 = 0.0489 - 0.0552i$	$b_7 = 0.0047 + 0.0045i$
$a_8 = 0.0472 + 0.0326i$	$b_8 = -0.0142 + 0.0137i$
$a_9 = -0.0280 - 0.0106i$	$b_9 = 0.0217 + 0.0163i$
$a_{10} = 0.0023 - 0.0093i$	$b_{10} = 0.0018 + 0.0018i$
$a_{11} = 0.0044i$	$b_{11} = -0.0245 - 0.0065i$
$a_{12} = 0.0067 - 0.0008i$	$b_{12} = 0.0030 - 0.0187i$
$a_{13} = -0.0001 - 0.0005i$	$b_{13} = -0.0002 - 0.0008i$
	$b_{14} = -0.0018 - 0.0138i$
	$b_{15} = 0.0194 - 0.0059i$
	$b_{16} = 0.0005 + 0.0062i$
	$b_{17} = -0.0036 + 0.0035i$
	$b_{18} = 0.0029 + 0.0032i$

Table 4: Coefficients of polynomials for  $5_2$  knot B

coefficients for $p_1(t)$	coefficients for $p_2(t)$
$a_1 = -0.1589 + 0.0574i$	$b_1 = 0.0680 + 0.0694i$
$a_2 = 0.0797 - 0.1159i$	$b_2 = 0.2410 - 0.2319i$
$a_3 = 0.0765 - 0.1082i$	$b_3 = 0.0416 + 0.1066i$
$a_4 = -0.0872 + 0.0842i$	$b_4 = -0.0063 - 0.0044i$
$a_5 = -0.0911 - 0.2192i$	$b_5 = 0.0004 - 0.0415i$
$a_6 = -0.1176 + 0.0255i$	$b_6 = 0.0619 + 0.0409i$
$a_7 = 0.0510 - 0.0117i$	$b_7 = -0.0308 + 0.0068i$
$a_8 = 0.0296 - 0.0560i$	$b_8 = -0.0123 + 0.0162i$
$a_9 = 0.0009 + 0.0291i$	$b_9 = 0.0056 + 0.0025i$
$a_{10} = 0.0085 + 0.0081i$	$b_{10} = 0.0050 + 0.0306i$
$a_{11} = -0.0141 - 0.0033i$	$b_{11} = -0.0117 - 0.0236i$
$a_{12} = 0.0297 + 0.0137i$	$b_{12} = 0.0062 - 0.0025i$
$a_{13} = -0.0043i$	$b_{13} = 0.0035 - 0.0057i$
$a_{14} = 0.0089 - 0.0009i$	$b_{14} = -0.0022 - 0.0069i$
$a_{15} = 0.0028 - 0.0035i$	$b_{15} = 0.0166 - 0.0156i$
	$b_{16} = -0.0055 + 0.0086i$
	$b_{17} = 0.0036 + 0.0024i$
	$b_{18} = -0.0055 - 0.0032i$
	$b_{19} = 0.0174 + 0.0059i$